International Research Journal of Engineering and Technology (IRJET) e-ISSN: 2395-0056
Volume: 05 Issue: 10 | Oct 2018 www.irjet.net p-ISSN: 2395-0072

Non-Linear Numerical Analysis of Pre-Cast Reinforced Concrete Dapped Ends Beams

A.Abdel-moniem[1], H. Madkour[2], A. Abdullah[2,3], K. Farah[2]

[1]*Researcher, Aswan University, Egypt*
[2]*Structural Engineering Department, Aswan University, Egypt*
[3]*Civil Engineering Department, Bisha University, Saudi Arabia.*

Abstract - *The analysis of dapped end beams often represents a problem due to the abrupt change in the geometry of it. A two-dimensional Finite element model using ABAQUS software has been built to study this problem. The aim of the research is numerically investigating the behavior of dapped end beams under static loading. The behavior of modelled specimens was validated based on previous experimental studies. The results showed that the present FE model at different steps was found to be agrees quite well with the previous test data.*

Key Words: Reinforced concrete; Dapped-end beams; Numerical investigation; Finite element; Shear failure.

1. INTRODUCTION

The developed shear and bending at the end of the beam should be carried by a small cross section. Moreover, the sudden change in geometry of the beam leads to high stress concentrations at the nib zone. Various cracks are happened due to the stress concentration at re-entrant corner and the damage due to corrosion increased. Leading to decrease the structure's life span or even compromises its safety. So that, the design of dapped ends requires special design. PCI design handbook [1] determined the five potential failure modes for dapped end as shown in fig. 1.

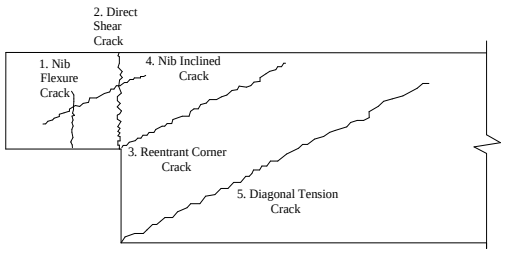

Fig-1: The main five potential failure cracks in dapped end beam [1].

The effect of dapped end beam geometry on the strength have been investigated by Wang et al. [2, 3]. He concluded that, the load capacity increases with decreasing the shear span to depth ratio and the nib height effect and recommended to not increasing the nib height to 0.45 from total height. In addition, he studied the load transfer for beams with shear span-to- depth ratio (a/d) not greater than unity [2, 4, 5]. Chung [6] investaged two shear span to depth (a/d) ratios, one less than 1.0 and one larger than 1.0, and the results were compared with the previous ones. While, the reinforcement ratio effect was investigated by using finite element programs [7-9]. The results of the finite elements studies concluded that the shear strength is affected by the shear span to depth ratio, concrete compressive strength, amount of nib reinforcements, and the amount of main reinforcement.

Gold et al. [10] experimentally tested dapped-end beams of a three-story parking garage strengthened by FRP plates that were insufficient in shear capacity. They verified their results by carrying out a series of tests to make sure of the predictive performance of their design approach. The results illustrated that the FRP strengthening systems increased the capacity of the beams.

Taher [11] experimentally studied 52 small-scale rectangular beams with many strengthening materials. FRP system was found to be the most suitable technique for strengthening and retrofitting applications. He also proposed a strut and tie model (STM) to estimate the capacity of the FRP-strengthened dapped-end beams, which seemingly provided "reasonable predictions". However, this model did not take into consideration the change in the size of the tested beams.

Tan [12] experimentally studied the effectiveness of many FRP arrangements for strengthening dapped-end beams with insufficient shear resistance, consisted of both fiber types and mechanical anchorage systems for FRPs. The results illustrated that glass fiber reinforced polymers (GFRP) given major improvements in ultimate capacity than carbon fiber polymers (CFRP) plates and carbon fiber fabrics.

On the other hand, Huang and Nanni [13] examined the increase in the dapped-end beams by using FRP systems. Atta et al. [14] proposed an experimental studies for the torsional behavior of recessed RC beams and discussed the FRP sheets, laminates and external pre-stressing steel applications under torsional moments. Gyorgy et al. [15] had proposed an experimental and numerical study of the efficiency of strengthening dapped-end reinforced concrete beams using externally bonded carbon fiber reinforced polymers.

2. VERFICITION SOURCES AND DATA

Some previous experimental results [11, 16] have been compared with numerical results to make a verification for the numerical model:

a) Her zinger [16], experimentally investigated dapped end beams with both conventional and studs reinforcement. The beam (B-A-1) from the experimental program was numerically modelled and named here (B-A-Ref.). The detailing of reinforcement for the tested beam are shown in Fig. 2.

b) Taher [11] experimentally studied specimens with dapped-ends. The beam (GI-0) from the experimental program was numerically modelled and named here (B-B-Ref.). The detailing of reinforcement for the tested beam are shown in Fig. 3.

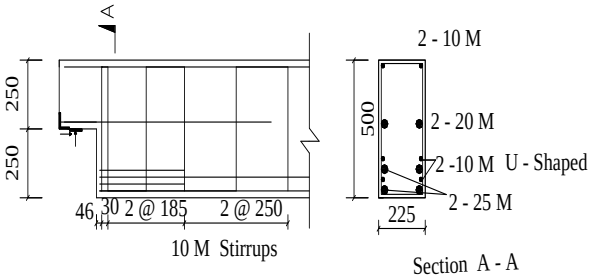

Fig-2: Reinforcement details of dapped end beam [16].

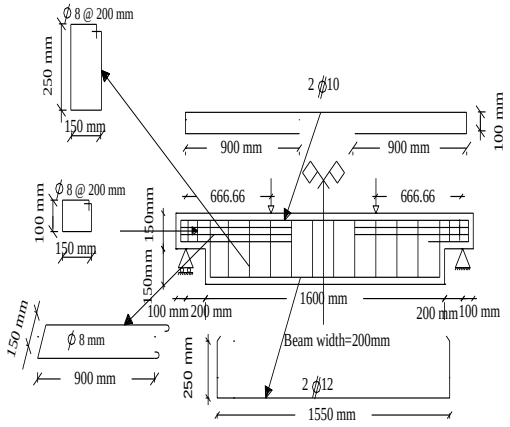

Fig-3: Reinforcement details of dapped end beam [11].

3. Finite Element Analysis

The ABAQUS program [17] has two main analysis modules: standard and explicit. ABAQUS/ standard uses an implicit strategy with an iterative equation solver to solve a large set of equation and approach the solution through successive equilibrium cycles. Therefore, ABAQUS/ standard is adopted here to model the concrete dapped end beam. While ABAQUS / explicit uses non-linear explicit dynamic formation and determines the solution by explicitly advancing the state of the model over minor increment without iteration.

3.1 Meshing element

The dapped end beam represented here as a two-dimensional (2D) plane stress continuum element because the thickness of the body is small relative to its lateral (in-plane) dimensions. The stresses are functions of planar coordinates alone, and the out-of-plane normal and shear stresses are equal to zero.

For concrete element in this study, we used four-node bilinear plane stress quadrilateral element (CPS4). Which, each node has two-dimensional translational degrees of freedom. Chart 1 show the difference between (CPS4) and reduced eight- node bilinear plane stress quadrilateral element (CPS8R) elements for concrete modelling. The two elements are usually used to modelling the concrete element in 2D- Modelling. In this research, the CPS4 element has been used.

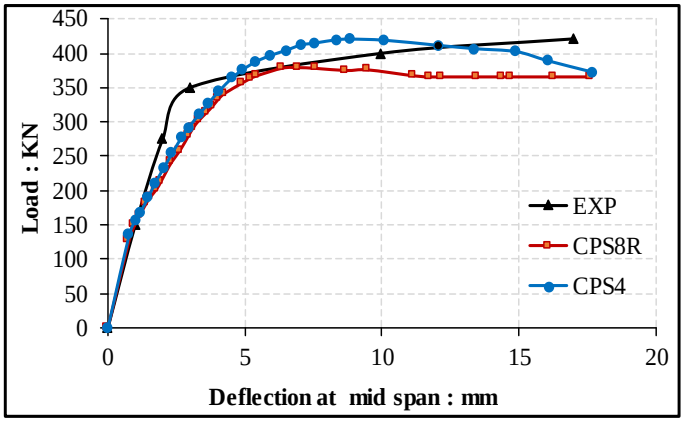

Chart-1: A comparison between CPS4 and CPS8R elements types for beam (B-A-Ref.).

For internal reinforcement, a two-dimensional two-node linear displacement (T2D2) truss element was used. These truss elements are embedded into "host continuum elements. Embedding means that the translational degrees of freedom at the nodes of the embedded element are discarded and turn off constrained to the corresponding distorted values in the host continuum element. The reinforcement-concrete interaction is not calculated, but is indirectly taken into account in the concrete model by modulating some portions of the plain concrete behavior. For modelling the supports of beam (hinged or roller) in this model we depended on a two dimensional rigid shell element which be determined as a model data and linked with a node, known as the rigid body reference node, whose motion dominates the motion of the surface.

3.2 Steps, increments, and iterations

The load history of the model contains three main steps, as follows:

1-Establish contact: the supports of the beam were modelled as a rigid surface to distribute the load over the supporting area, and to permit the beam to pick up. Therefore, a contact definition was needed before applying the loads.
2- Release constraints: this step is a consequence of the prior step.
3- Loading: displacement increments are used pending to failure in this step. The experimental maximum displacement values have been used in models.

3.3 Materials Models

3.3.1 Steel Reinforcement

The steel reinforcement was determined relying on the stress-strain curve of the uniaxial tensile tests. The behavior was represented as a bilinear curve (linear elastic with strain hardening). The elastic part of the behavior was determined by the longitudinal elastic modulus and Poison's ratio. The steel reinforcement material properties are illustrated in Table 1.

3.3.2 Concrete

ABAQUS provides the capability of simulating the damage using either of the two crack models for reinforced concrete elements: (1) Smeared crack concrete model, In addition (2) Concrete damaged plasticity model. Out of the two concrete crack models, the concrete damaged plasticity model is selected in the present study as this technique has the potential to represent complete inelastic behavior of concrete both in tension and compression. While the smeared cracking has an early upon crack detection, makes the analysis stop due to numerical stability after a very small deflection, as shown in chart 2.

Table-1: Steel reinforcement material properties for the proposed models.

Property	Unit	Value
Yield stress for steel rebars	MPA	400
Ultimate stress for steel rebars	MPA	600
Yield stress for steel stirrups	MPA	280
Yield stress for steel stirrups	MPA	250
Steel modulus of elasticity	MPA	191500
Steel Poisson's ratio	MPA	0.3

Table-2: Concrete material properties for the proposed model.

Property	Unit	Value
Group (A)		
concrete compressive strength	MPA	38
Concrete modulus of elasticity	MPA	29000
Concrete Poisson's ratio	-	0.18
Maximum compressive and tensile strain	-	0.0035
Tensile strength (F_{ctk})	MPA	2.40
Group (B)		
concrete compressive strength	MPA	25
Concrete modulus of elasticity	MPA	22000
`Concrete Poisson's ratio	-	0.18
Maximum compressive and tensile strain	-	0.0035
Tensile strength (F_{ctk})	MPA	1.80

The CDP (Concrete Damaged Plasticity) model makes use of the yield function of Lubliner et.al. [18], with modifications proposed by Lee and Fenves [19] to explicate various evolution of strength under tension and compression. The damaged plasticity assumes a non-associated flow rule to determine the flow potential, which is based on the Drucker- Prager hyperbolic function [20].

The concrete properties are illustrated in table 2. The material model for concrete under compression taken from Eurocode 2, part 1.1 [21], and it modulated to comprise the initial linear elastic response up to 40% of the mean Compressive strength as shown in chart 3-b. The mean compressive strength ($F_{cm}=F_{ck}+8$) of concrete was taken as the peak compressive strength, where (F_{ck}) is the characteristic compressive strength of concrete. While the tensile behavior of concrete is given here by an approach proposed by Scanlon [22]. Scanlon's parataxis for the tension-stiffening curve of concrete is shown in chart 3-a.

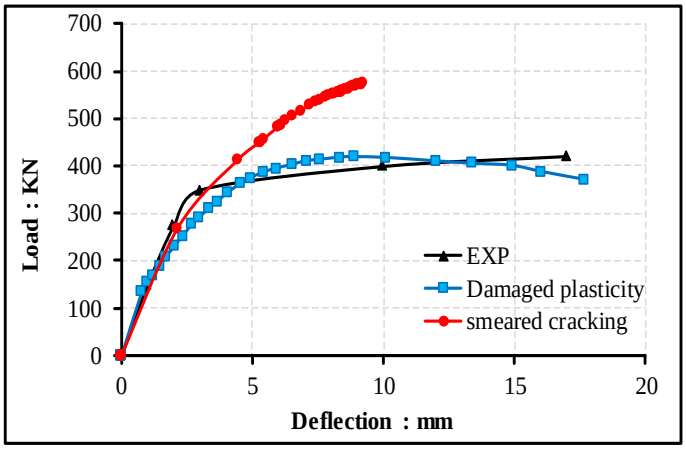

Chart-2: load-deflection curve for Smeared cracking and damaged plasticity models.

3.4 Description of dapped end beam model

A dimensional (2D) plane- stress continuum element is used to model the dapped end beam. Half of the beam length is adopted in the modelling program, because the beam is symmetry. The modelled beams consists of the following parts as shown in fig. 4: concrete, horizontal reinforcement, vertical stirrups, and support.

To simulate the contact between the beam surface and the rigid surface chosen for supports a simple contact algorithm is defined by specifying the interaction between the contacting surfaces [23] as shown in fig. 4. This interaction was taken tangential to the surfaces. The tangential component, which consists of the relative motion of the surfaces, was assumed frictionless, since this is the common assumption in simply supported members. The normal behavior applies the contact constrains only when the clearance between two surfaces becomes zero. In such case, the accumulation of the contact pressure transmitted from the beam element to the rigid surface is equal to the applied load (reaction). The surfaces separate when the contact pressure between them becomes zero or negative, and the constraint is removed. This method is more appropriate than the method of releasing predetermined nodes near the beam ends, as the latter method requires iterative process to identify these nodes.

3.5.1 Mesh Size

Mesh sensitive may not considered in reinforced concrete elements with reasonably distributed cracks if the element aspect ratio is near unity. However, if the failure mode of the structural element is described by crack localization in certain areas, mesh density is yet a critical problem Therefore, mesh sensitivity was investigated. For this purpose, the reference beam (B-A-Ref) [16], was considered in order to study the effect of mesh size. For concrete we considered Scanlon tension stiffening curve [22]. The tensile strength was taken as the mean value F_{ctm} defined in Eurocode 2 [21].

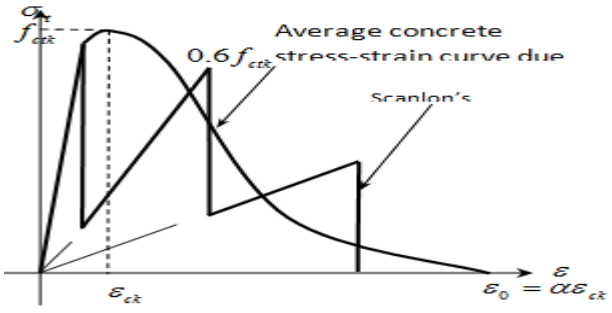

(a)

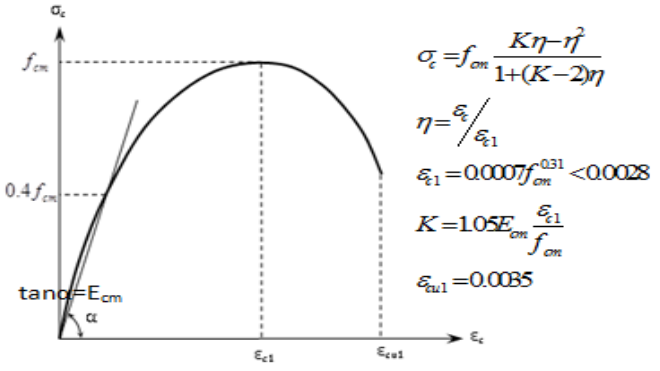

(b)

Chart-3: Concrete behavior under uniaxial loading in, a) tension, b) compression.

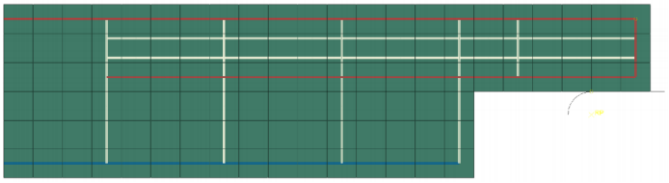

Fig. 4: The elements of beam model.

Different mesh sizes were considered in the sensitivity analysis so that the tension stiffening overshadows softening of concrete. This was achieved by keeping the crack band width, h, for each mesh size less than the characteristic length of concrete, $\lambda = 2G_f E / f_{ck}^2$. The nominal mesh sizes considered were 50, 62.5, 100, and 125 mm, and the element is kept as close to cube, as possible.

Based on the previously results shown in the chart 4, the convergence study for beam (B-A-Ref) implies that the 62.5 mm mesh size is most suitable size. Therefore, it was decided to adopt the 62.5 mm mesh size for the rest of the analysis of beams group (A).While, for beams of group (B) the change in mesh size also gave convergent results. Therefore, the 50 mm mesh size was adopted in the analysis for achieving a cube element shape.

3.5.2 Effect of tension stiffening curve

Different tension stiffening models are compared in this study to get the best model that describes well the post-cracking behaviour of concrete. The models includes linear, bi-linear, and Scanlon [22, 24-26]. In addition to Collins & Mitchell, Okamura, Crvenkas models [27-31].

The tensile strength was taken as the mean bound defined in Eurocode 2 [21], F_{ctm}. The strength criterion was adopted for all beams. The load deflection curve for beam (B-A-Ref.) is shown in chart 5. Consequently, Scanlon's model was adopted for conducting the analysis of the test beams.

In conclusion, the approach of tension stiffening with reduced tensile concrete strength was used in the FE analyses of the test beams. Scanlon's approach was used with appropriate terminal strain, ε_0. This terminal strain was "calibrated" based on the load deflection response of each test.

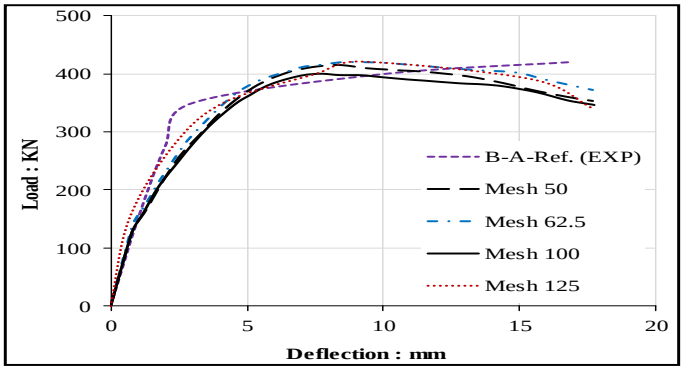

Chart-4: mesh sensitivity of beam (B-A-REF.).

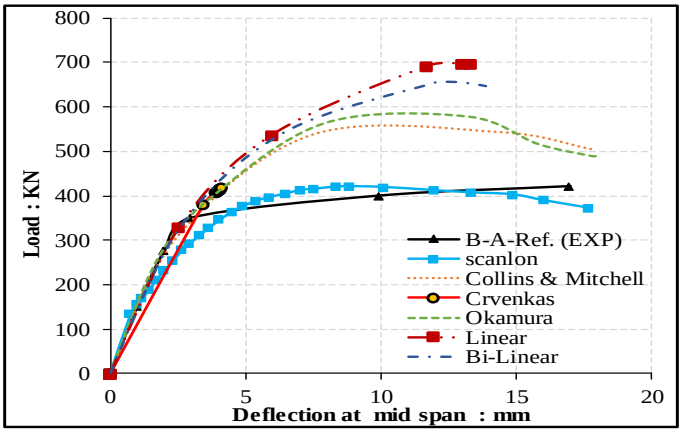

Chart-5: load-deflection curve of beam (B-A-REF) with different tension stiffening models.

4. Results and Discussion

Chart 6 show the load–deflection curves for the two reinforced concrete dapped-end beams (B-A-Ref.) and (B-B-Ref.) proposed by the present finite element model are compared with previous experimental results [11, 16].

For the dapped-end beam (B-A-Ref.), the load-Deflection curve shown in chart 5, the ultimate loads from the finite element and experimental models are 420.64kN and 421kN, respectively, the cracking loads are 135.7KN and 150KN, and the ultimate deflection are 17.69mm, and 17mm, respectively. For dapped-end beam (B-B-Ref.), the ultimate loads from the finite element and experimental models are 80.87kN and 75kN, respectively, the cracking loads are 23.53KN and 25KN, and the ultimate deflection are 18.9mm, and 18mm, respectively. In general, the numerical load-deflection curves presented here concur to a large degree with the previous experimental data of Ref. [11, 16]. However, the finite element load-deflection curve is slightly unlike the experimental curve. Many reasons may explain this case. First, micro cracks that happen in the concrete for the tested beam due to drying shrinkage in the concrete and/or handling of the beam. While, the finite element models do not contain the micro cracks. The second reason is the perfect bond between the concrete and steel reinforcements in the finite element analysis is proposed.

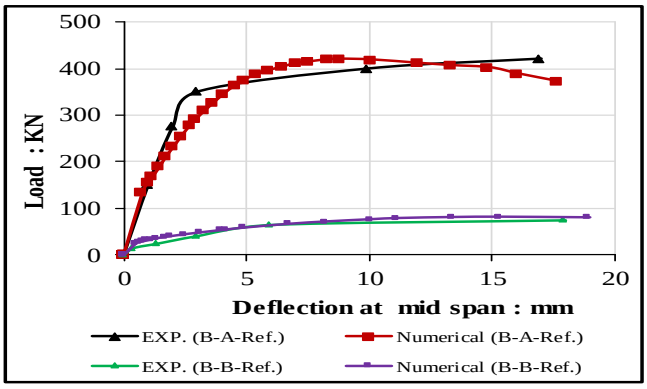

Chart-6: Numerical load – Deflection curve compared with experimental results [11, 16].

5. CONCLUSION

A Finite element model has been built to imitate the behavior of RC dapped-end beams under static monotonic loading. The model takes into consideration the linear and nonlinear properties for concrete and steel. The numerical results proposed from the FE model then compared with the previous tests data to have a good verification. The results showed that, the predicted loads, and deflections of the reinforced concrete dapped-end beams by the present FE models at various stages were found to be agrees well with the previous test data. In addition, some parameters such as tension stiffening effect, mesh sensitivity effect have been studied.

REFERENCES

[1] P. I. H. Committee, "PCI design handbook: precast and prestressed concrete," ed: MNL-120. 6th ed. Chicago, IL: PCI, 2006.

[2] Q. Wang, Z. Guo, and P. C. Hoogenboom, "Experimental investigation on the shear capacity of RC dapped end beams and design recommendations," Structural Engineering and Mechanics, vol. 21, p. 221, 2005.

[3] I.-J. Lin, S.-J. Hwang, W.-Y. Lu, and J.-T. Tsai, "Shear strength of reinforced concrete dapped-end beams," Structural Engineering and Mechanics, vol. 16, pp. 275-294, 2003.

[4] A. H. Mattock and T. C. Chan, "Design and behavior of dapped-end beams," PCI Journal, vol. 24, pp. 28-45, 1979.

[5] K.-H. Yang, A. F. Ashour, and J. Lee, "Shear strength of reinforced concrete dapped-end beams using mechanism analysis," 2011.

[6] J. C.-j. Chung, "Effect of depth of nib on strength of a dapped-end beam," University of Washington, 1985.

[7] M. Aswin, B. S. Mohammed, M. S. Liew, and Z. I. Syed, "Shear failure of RC dapped-end beams," Advances in Materials science and engineering, vol. 2015, 2015.

[8] J. Y. Moreno, "Experimental study and numerical simulation of the behaviour of concrete dapped-e beams," International Journal for Engineering Modelling, vol. 26, 2013.

[9] A. Mohammed, "Nonlinear Three-Dimensional Finite Element Analysis of Reinforced Concrete Dapped-End Beams," iraqi journal of civil engineering, vol. 9(1), pp. 1-16, 2011.

[10] W. J. Gold, G. J. Blaszak, M. Mettemeyer, A. Nanni, and M. D. Wuerthele, "Strengthening dapped ends of precast double tees with externally bonded FRP reinforcement," in Advanced Technology in Structural Engineering, ed, 2000, pp. 1-9.

[11] S.-D. Taher, "Strengthening of critically designed girders with dapped ends," Proceedings of the Institution of Civil Engineers-Structures and Buildings, vol. 158, pp. 141-152, 2005.

[12] K. H. Tan, "Shear strengthening of dapped beams using FRP systems," in FRPRCS-5: Fibre-reinforced plastics for reinforced concrete structures Volume 1:

Proceedings of the fifth international conference on fibre-reinforced plastics for reinforced concrete structures, Cambridge, UK, 16–18 July 2001, 2001, pp. 249-258.

[13] P.-C. Huang and A. Nanni, "Dapped-end strengthening of full-scale prestressed double tee beams with FRP composites," Advances in Structural Engineering, vol. 9, pp. 293-308, 2006.

[14] A. M. Atta and T. F. El-Shafiey, "Strengthening of RC dapped-end beams under torsional moment," Magazine of Concrete Research, vol. 66, pp. 1065-1072, 2014.

[15] T. Nagy-György, G. Sas, A. Dăescu, J. A. Barros, and V. Stoian, "Experimental and numerical assessment of the effectiveness of FRP-based strengthening configurations for dapped-end RC beams," Engineering structures, vol. 44, pp. 291-303, 2012.

[16] R. Herzinger, "Stud reinforcement in dapped ends of concrete beams," presented at the AICSGE 5, At Alexandria, Egypt, 2008.

[17] U. m. ABAQUS, "Version 6.10.," in ABAQUS Documentation, ed.

[18] J. Lubliner, J. Oliver, S. Oller, and E. Onate, "A plastic-damage model for concrete," International Journal of solids and structures, vol. 25, pp. 299-326, 1989.

[19] J. Lee and G. L. Fenves, "Plastic-damage model for cyclic loading of concrete structures," Journal of engineering mechanics, vol. 124, pp. 892-900, 1998.

[20] H. Madkour, "Non-linear analysis of strengthened RC beams with web openings," Proceedings of the Institution of Civil Engineers-Structures and Buildings, vol. 162, pp. 115-128, 2009.

[21] A. Committee, A. C. Institute, and I. O. f. Standardization, "Building code requirements for structural concrete (ACI 318-14) and commentary," 2014.

[22] A. Scanlon and D. W. Murray, "Time-dependent reinforced concrete slab deflections," Journal of the Structural Division, vol. 100, 1974.

[23] A. M. Abdullah and C. Bailey, Analysis of repaired/strengthened RC structures using composite materials: punching shear: University of Manchester, 2010.

[24] V. Cervenka, L. Jendele, and J. Cervenka, "ATENA program documentation, Part 1: Theory," Cervenka Consulting, Prague, vol. 231, 2007.

[25] H. Cornelissen, D. Hordijk, and H. Reinhardt, "Experimental determination of crack softening characteristics of normalweight and lightweight," Heron, vol. 31, p. 45, 1986.

[26] F. Barzegar and W. C. Schnobrich, "Post-cracking analysis of reinforced concrete panels including tension stiffening," Canadian Journal of Civil Engineering, vol. 17, pp. 311-320, 1990.

[27] P. Valerio and T. J. Ibell, "Shear strengthening of existing concrete bridges," Proceedings of the Institution of Civil Engineers-Structures and Buildings, vol. 156, pp. 75-84, 2003.

[28] T. Telford, "CEB-FIP Modelcode 1990," European Design Code, Lausanne, Switzerland, 1993.

[29] P. C. Huang, Myers, J.J., and Nanni, A.,. (2000). Dapped-end strengthening of precast prestressed concrete double tee beams with FRP composites.

[30] E. Hognestad, "Study of combined bending and axial load in reinforced concrete members," University of Illinois at Urbana Champaign, College of Engineering. Engineering Experiment Station.1951.

[31] L. P. Saenz, "Equation for the stress-strain curve of concrete," ACI Jour., vol. 61, pp. 1229-235, 1964.